Long Term Monitoring of Air Pollution on Monuments and Cultural Heritage Sites in Cyprus Using Satellite Remote Sensing

K. Themistocleous*[a], A. Nisantzi[a], A. Agapiou[a], D. D. Alexakis[a], D. G. Hadjimitsis[a], V. Lysandrou[b], S. Perdikou[c], A. Retalis[d], N. Chrysoulakis[e]

[a]Department of Civil Engineering & Geomatics, Cyprus University of Technology, Lemesos, Cyprus
(k.themistocleous, argyro.nisantzi, athos.agapiou, dimitrios.alexakis, d.hadjimitsis)@cut.ac.cy.

[b]Restoration of Monuments and Sites, Kykkos Museum,
vaslysandrou@yahoo.it

[c]Department of Civil Engineering, Frederick University, Nicosia, Cyprus
skevi@mail.com

[d]Institute of Environmental Research and Sustainable Development, National Observatory of Athens, Greece,
adrianr@meteo.noa.gr.

[e]Institute of Applied and Computational Mathematics, Foundation for Research and Technology - Heraklion, Crete, Greece,
zedd2@iacm.forth.gr

*Corresponding author.

Long Term Monitoring of Air Pollution on Monuments and Cultural Heritage Sites in Cyprus Using Satellite Remote Sensing

K. Themistocleous, A. Nisantzi, A. Agapiou, D. D. Alexakis, D. G. Hadjimitsis, V. Lysandrou, S. Perdikou, A. Retalis, N. Chrysoulakis

Abstract

Although cultural heritage sites are documented and preserved, to date there has been limited monitoring and documentation of how cultural heritage sites are affected by air pollution. This paper aims to introduce a new approach for monitoring air pollution for areas near cultural heritage sites by using satellite remotely sensed data. This approach provides a cost-effective tool for local authorities and government agencies to identify the most polluted cultural heritage sites and make decisions regarding the conservation of these sites. Archived data may be used in order to study long term the impact of air pollution to cultural heritage sites. The study area includes significant open air monuments of Cyprus located in the four main cities of the island. In this paper the Limassol Castle is used as a focused case study. Three years of MODIS satellite data was evaluated and analyzed in order to categorize high risk long-term areas. Ground measurements using sun-photometers, spectro-radiometers and particulate matter (PM10) laser photometer were also utilized in the study. The darkest pixel atmospheric correction in conjunction with the use of the radiative transfer equation was applied to retrieve the aerosol optical thickness (AOT) from Landsat TM/ETM+ satellite images in order also to cross-validate the AOT values found from MODIS and sun-photometers. The results of the study

indicate that air pollution is high in all the major cities in Cyprus near cultural heritage sites. The results also found that the Limassol castle was most affected by air pollution, while the other cultural heritage sites exhibited similar results.

KEY WORDS: monitoring air pollution, PM measurements, MODIS, AOT, cultural heritage, remote sensing, GIS

1. INTRODUCTION

1.1 Monitoring air pollution

Atmospheric pollution is widely recognised as one of the major threats to cultural heritage sites (Navas et al.,2010). Atmospheric pollution causes damage to cultural heritage sites, including soiling, material deterioration due to chemical reactions, and increased stone decay (Reyes et al., 2011). Therefore, knowledge of atmospheric aerosol composition near monuments has become an increasingly important issue in preservation strategies (Ghedini et al., 2011)

However, monitoring air pollution is not an easy task. According to Ferradás et al. (2010), the EC Directive, 2008 (2008/50/EC) permits a maximum expanded uncertainty of 15-25% for methods using fixed monitors, depending on the pollutant in question, whereas indicative measurements and modelling techniques have wider margins of error of up to 25-50%. In order to record air pollutant, a network of ground samples is usually set up in the area of interest (Pummakarnchana et al., 2005; Pfeffer et al. 1995), yet such methods are expensive to implement and maintain and are also spatially limited (Ferradás et al. 2010). Due to their spatial and temporal variability, atmospheric aerosol monitoring is difficult and efforts to improve aerosol characterizations have included using in-situ measurements, ground-based remote sensing and satellite observations (Themistocleous et al., 2011).

Satellite remote sensing is an excellent non-evasive tool that can be used to monitor pollution and its effects both temporally and spatially. Spectral variations recorded by satellite sensors are indicators of aerosol particles and, therefore, air pollution. When solar radiation travels through the atmosphere, it produces a general decrease in the spectral irradiance which is related to the optical thickness of the atmosphere. These effects are due to the scattering and wide band

absorption produced by both aerosol particles and atmospheric gases (Pujadas et al., 2000)

Several studies have shown that satellite data can be used to monitor air pollution and air pollution effects. Tømmervik et al. (1995) compared vegetation cover maps and air pollution emissions data over a 15 year period and found major changes in the environment as a result of high air pollution values. Nisantzi et al. (2011) used MODIS satellite data to analyse the relationship between the aerosol optical thickness (AOT) and the PM_{10} as indicators of pollution.

AOT represents the extinction of incoming solar radiation by aerosols over the atmospheric column and it is related to aerosol concentration, and vertical profile of the aerosol extinction coefficient. AOT can be retrieved from numerous sensors, including the Moderate Resolution Imaging Spectroradiometer (MODIS) (Péré, et al., 2009), which is used in this study. The MODIS sensor has 36 different channels with varying spatial resolution of 250, 500 and 1000 m. The spectral range of the sensor extends from 410 to 14,200 nm. Aerosol retrievals over land from MODIS are described originally by Kaufman et al. (1997). Two independent retrievals are conducted at 470 and 660 nm, and subsequently interpolated to 550 nm. The surface reflectance for the channels at 470 and 660 nm are estimated from measurements at 2.1 μm using empirical relationships. Geographically and seasonally varying multimodal aerosol models are assumed (Martin, 2008). Uncertainty above land is given by 0.05 + 0.2 × AOT (Kaufman et al., 1997). Péré, et al. (2009) conducted a correlation of MODIS and ground PM10 measurements, with a correlation coefficient (R) between 0.68 - 0.79.

1.2 AOT measurements

The key parameter for assessing atmospheric pollution in air pollution studies is the aerosol optical thickness. Aerosol optical thickness (AOT) is a measure of aerosol loading in the atmosphere (Retails et al., 2010). High AOT values suggest high concentration of aerosols, and therefore air pollution (Retalis et al, 2010). The use of earth observation is based on the monitoring and determination of AOT either direct or indirect as tool for assessing and measure air pollution. Measurements on PM10 and PM2.5 are found to be related with the AOT values as shown by Lee et al. (2011), Hadjimitsis et al. (2010), Nisantzi et al. (2011). Hadjimitsis (2008), Hadjimitsis and Clayton (2009) and Hadjimitsis (2009) used indirect method for retrieving AOT using atmospheric correction method and radiative transfer equation intended for the use of Landsat TM/ETM+ and ASTER imagery. Themistocleous et al. (2010) used AOT data to examine the air pollution near to cultural heritage sites in the centre of Limassol area in Cyprus. Themistocleous et al.

(2011) presented the results obtained by using Landsat TM/ETM+ imagery over Limassol using the darkest pixel atmospheric correction method for retrieving the AOT values. Nisantzi et al. (2011) used both particulate matter (PM10) device, backscattering lidar system, AERONET and hand-held sun-photometers for investigating PM10 against MODIS AOT regression model over the urban area of Limassol in Cyprus.

1.3 Impact of air pollution on monuments

Cultural heritage sites can be damaged in various ways through the long term processes and deterioration mechanisms associated with air pollutants. For example, pollutants such as SOx, NOx, CO2 dissolved in rainwater to create acid rain which produce a hive form degradation or acupuncture corrosion on historical sites (Kozaris and Kefala,1989). Moreover, air pollutants provoke corrosion on the stone, causing an aesthetic effect on the surfaces and details of monuments. The deposits of air pollutants on the surface of the monuments result in the creation of black or other crust depending on the components of air pollutants etc. As well, air pollution can also weaken the binder of the joints of stone buildings and also result in a loss of material from the joints. More delicate surfaces, such as frescoes, that are exposed to the polluted atmosphere (such as the case of the archaeological site 'Tomb of the Kings' at Nea Paphos Fig.2) experience a surface weakening, progressive pulverization and also the creation of a hydroscopic layer of gypsum on the surface of the fresco.

Although the above effects are refer to slow deterioration actions, they may cause irreversible problems in the long term that will prevent the proper salvation of the monument (Skoulikides, 2000). Therefore, improving air quality is critical for the preservation and maintenance of cultural heritage sites. This study presents a combination of non-evasive tools that can be used remotely to monitor pollution in order to prevent further destruction. These tools can be used by local authorities and government agencies to measure air pollution, in order to make appropriate decisions to decrease the level of pollution around cultural heritage sites and therefore prevent further destruction.

1.4 Case study area

Many pre-historical and historical monuments are found in Cyprus. This study focuses on significant cultural heritage sites located in the four major cities in Cyprus (Figure 1). These sites are the "Nea Paphos" and the "Tombs of the Kings" sites (Paphos district), which are listed as world heritage monuments by UNESCO, the archaeological site

"Kition" in Larnaca district, the dozen of monuments which are within the old walls of Nicosia and the "Medieval Castle" of Limassol, located at the center of the town (Figure 2). The case study of the Limassol castle will be presented in this paper.

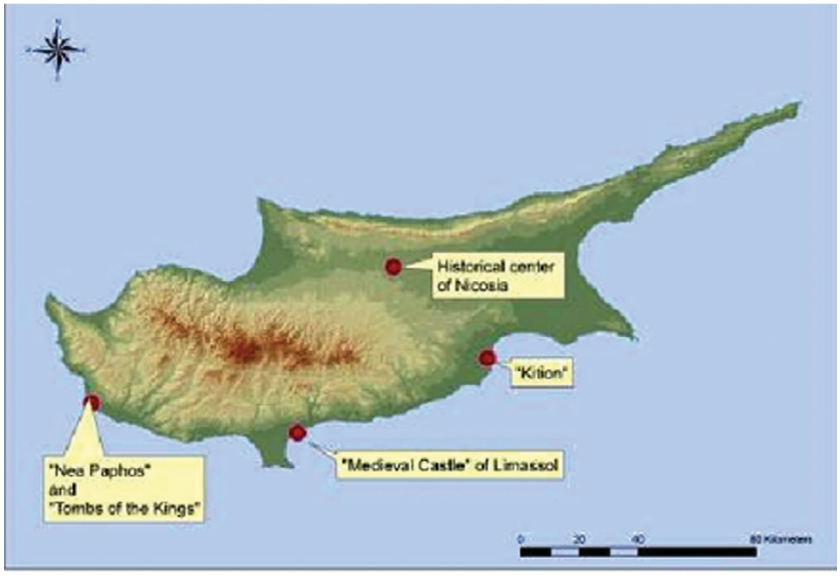

Figure 1: Selected monuments for the aims of the study.

Figure 2: Selected archaeological sites: "Tombs of the Kings" (top left); "Kition" (top right); "Nea Paphos" (lower left) and "Medieval Castle" of Limassol (lower right).

The Limassol Castle was built in the 14th century on the site of an earlier Byzantine Castle, where Richard the Lionheart, King of England, married Princess Berengaria of Navarre in 1191 and crowned her Queen of England. According to Etienne Lusignan, the original Castle was erected by Guy de Lusignan in 1193 and was surrendered to the Knights of Jerusalem in 1308. Archaeological excavations within the Castle exposed a marble podium from an early Christian basilica and the floor of a Middle Byzantine monument from the 10th or 11th century. In 1373, the Genoese burned down Limassol town after having occupied the Castle. It is likely that the Castle was badly damaged. The Castle was again restored in order to withstand renewed attacks by the Genoese in 1402 and 1408. In 1413, the Castle survived the first attack of the Mamluks but severe damage resulting from an earthquake led to its capture in 1425 by the Mamluks in their second attack on the city. At the beginning of the 16th century, extensive reconstruction took place. The gothic arches of the underground chamber and the openings in the side walls can be attributed to this period. The castle is a significant tourist attraction all year round (Cyprus Department of Antiquities, 2011).

2. Methodology and Resources

This study utilized a variety of remote sensing tool to measure air pollution. Satellite images such as Landsat TM/ETM+ and MODIS were used to directly or indirectly retrieve AOT, as were ground measurements using sun-photometers and spectro-radiometers. Further, air particles measurements were correlated to the AOT levels to verify the level of pollution. Last, visual observation of the Limassol Castle identified the damage caused by air pollution and laser scanning to document and monitor the damage was conducted.

2.1 Methodology

Remote sensing data was used in order to retrieve AOT for a period of 3 years (2009-2011). MODIS AOT values over the cultural heritage sites of interest were extracted from a GIS environment (ArcGIS v.10). AOT values were analyzed and correlated with air pollution in order to detect the risk of the open air to monuments. The results were verified with ground samplers' measurements while visual interpretation was carried out in some of the monuments (Figure 4).

2.2 Satellite Data

Monitoring air quality for each archaeological site using conventional methods is difficult and expensive. Air pollution

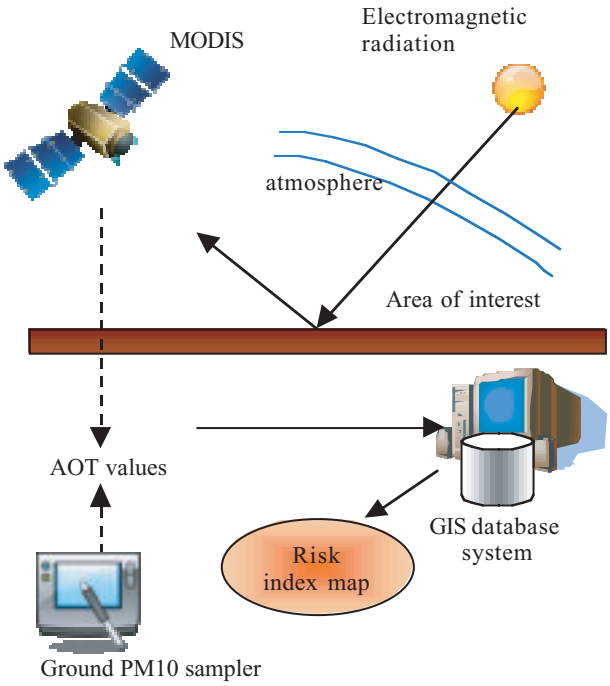

Figure 3: Methodology applied for monitoring air pollution using remote sensing data

measurements taken by air quality stations are often too far from the area and the monument of interest. In order to be able to effectively monitor air pollution, remote sensing images that provide daily values of AOT can be used. Such images cover a vast area and they can provide also historical data. In this study, MODIS data were used (Figure 4 and Figure 5).

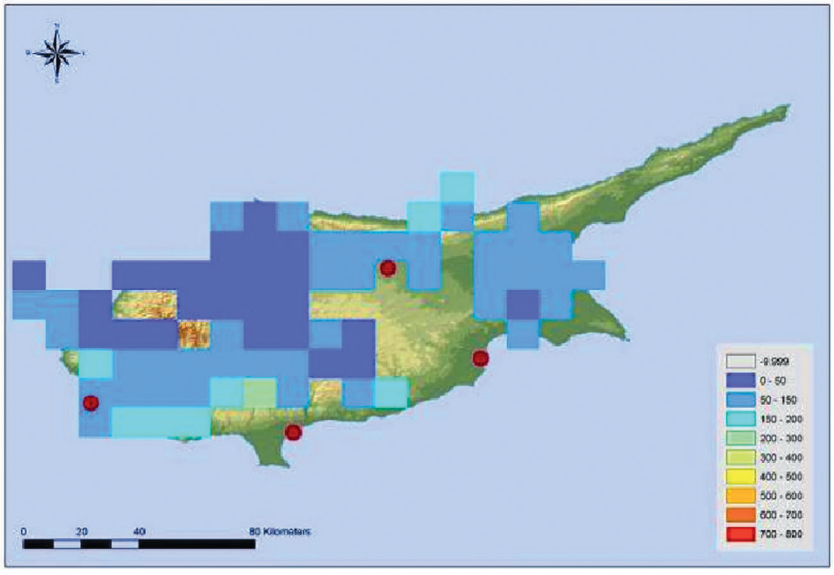

Figure 5: MODIS Aerosol Optical Thickness over Cyprus (02-02-2011) (value scale 0.01).

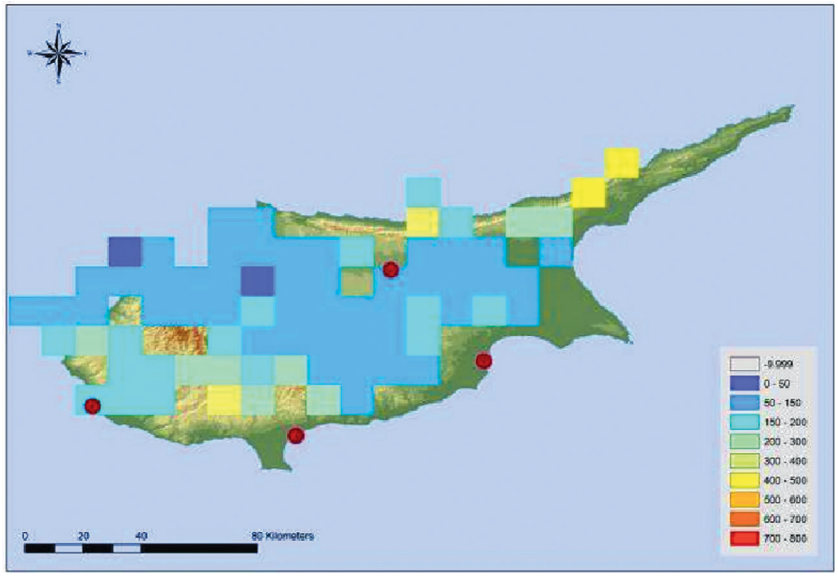

Figure 6: MODIS Aerosol Optical Thickness over Cyprus (18-02-2011) (value scale 0.01).

The MODIS Aerosol Product (MOD 04) monitors the ambient aerosol optical thickness over the oceans globally and over a portion of the continents. Furthermore, the aerosol size distribution is derived over the oceans, and the aerosol type is derived over the continents. Daily Level 2 (MOD 04) data are produced at the spatial resolution of a 10 _ 10 1-km (at nadir)-pixel array (HandBook MODIS).

In this study, over 900 satellite images, ranging from 2009 until 2011, were downloaded from the USGS database. After the necessary geometric transformation of all the data to the World Geodetic System (WGS '84) the AOT values were extracted in the ArcGIS environment and the major archaeological sites and monuments were also digitized along with the urban limits of Cyprus and the major road network.

Landsat TM/ETM+ imagery were also used to retrieve AOT values through the application of the darkest pixel atmospheric correction.

2.3 Ground Measurements

2.3.1 Sun-Photometers

Two sun photometers were used to retrieve AOT (at 500nm). The Cimel sun-photometer (Figure 6) is an automatic sun-sky scanning radiometer which can measure the direct solar irradiance at eight solar spectral bands and sky radiance at four of those wavelengths at the Earth's surface. The CIMEL sun-photometer is part of the AErosol RObotic NETwork (AERONET) and is calibrated according to program of AERONET specifications (Holben et al., 1998). The Microtops II (Figure 7) is a hand-held sun-photometer which measures the attenuation of the

direct solar irradiance and the transmittance from which AOT of the atmosphere is derived (Tsanev and Mather, 2008).

Figure 6: CIMEL SUN-PHOTOMETER (Cyprus University of Technology Premises-Remote Sensing Lab)

Figure 7: Hand-held Sun photometer - Microtops II (Cyprus University of Technology Premises-Remote Sensing Lab)

2.3.2 PM10 measurements

A PM10 DustTrack was also used in order to measure the PM mass. The TSI DustTrak is a light scattering laser photometer which measures the amount of scattering light relative to volume concentrations of

aerosols to obtain the mass concentration. The instrument is placed in the environmental enclosure and is mounted to a standard surveyor tripod for allowing reliable and accurate sampling.

3. Results

3.1 MODIS AOT measurements

The AOT measurement derived from the MODIS satellite were measured for the heritage sites located in the four major cities across Cyprus. It was found that the AOT levels at all sites was above the air quality 'AOT threshold=300' (i.e AOT=0.300) found from other studies using empirical approach such as the use of linear regression models between AOT Vs PM10 (Hadjimitsis et al., 2010). The case study of the Limassol Castle (Figure 8, Figure 12) indicated that the Limassol Castle has the highest values of all the sites across the island. Of the 35 MODIS images used for retrieving AOT values, 85% of the measurements exceeded the air quality threshold, indicating that the Castle is located in a polluted area. The Castle in the center of the city, in close proximity with the old port of Limassol and it is surrounded by roads with heavy traffic.

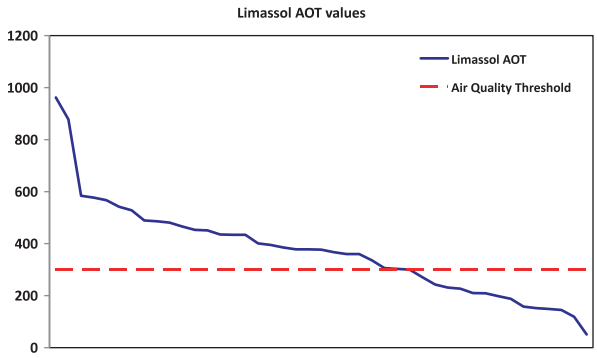

Figure 8: Limassol AOT values (sample = 35 measurements) in blue color. In red circle is the threshold air quality limit of 300 (AOT 0.300). In the y-axis, AOT value is multiplied by 1000 (to match MODIS data)

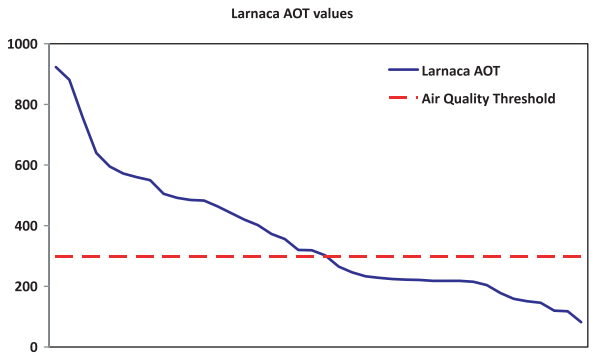

Figure 9: Larnaca AOT values (sample = 41 measurements) in blue color. In red circle is the threshold air quality limit of 300 (AOT 0.300). In the y-axis, AOT value is multiplied by 1000 (to match MODIS data)

Similar air quality results were found for the remaining heritage sites in the study. Larnaca, Paphos and Nicosia had a 53%, 54% and 49% measurements above the threshold of AOT 300 (AOT 0.300) (Figure 9 to Figure 12). This analysis suggest that cultural heritage sites are exposed to air pollutants half the time.

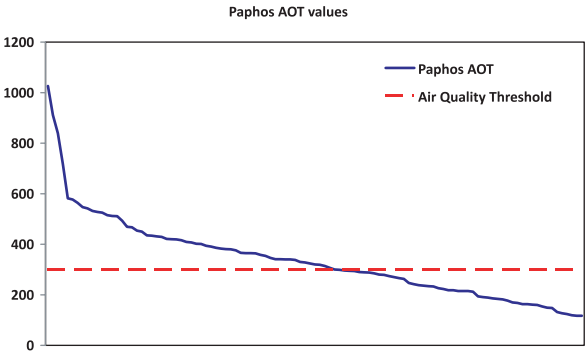

Figure 10: Paphos AOT values (sample = 109 measurements) in blue color. In red circle is the threshold air quality limit of 300 (AOT 0.300). In the y-axis, AOT value is multiplied by 1000 (to match MODIS data)

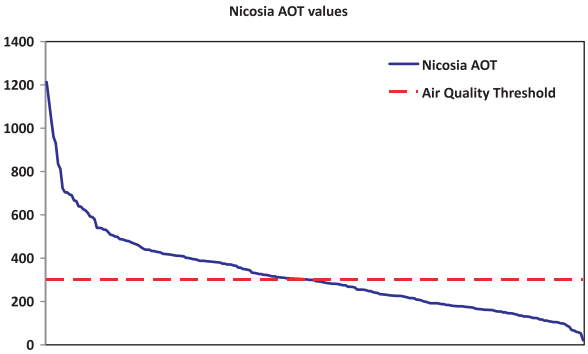

Figure 11: Nicosia AOT values (sample = 236 measurements) in blue color. In red circle is the threshold air quality limit of 300 (AOT=0.300). In the y-axis, AOT value is multiplied by 1000 (to match MODIS data)

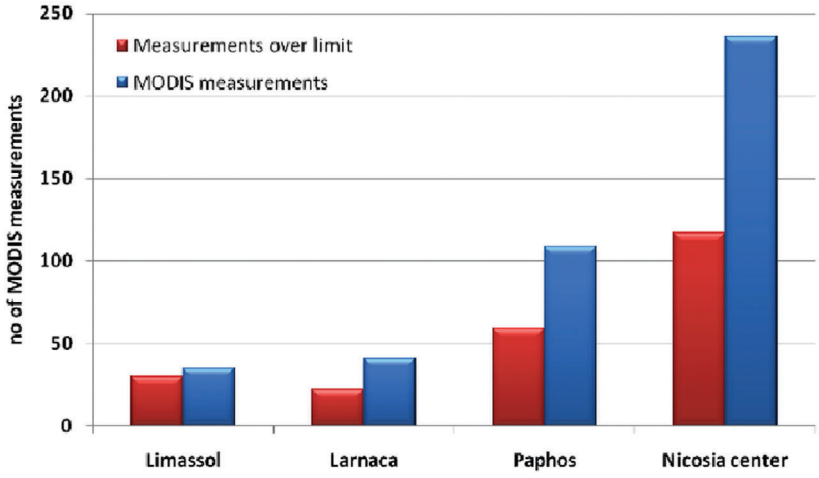

Figure 12: Overall measurements from MODIS images (blue bar) and measurements over the threshold limit (red bars).

3.2 PM10 Measurements

Ground PM10 measurements were highly correlated with the AOT values derived from ground measurements and the AOT derived from the satellite. A linear correlation coefficient (R2) between AOT values from ground measurements (AERONET) and AOT retrieval from MODIS data was 0.822 for Limassol area. MODIS data have shown also similar linear correlation coefficient (R2) with sun-photometer data (R2=0.867). In correlating AOT values with PM10 measurements, there was a linear correlation coefficient (R2) of 0.55 between the CIMEL sun photometer and the PM measurements (Figure 13) (Nisantzi et al., 2011).

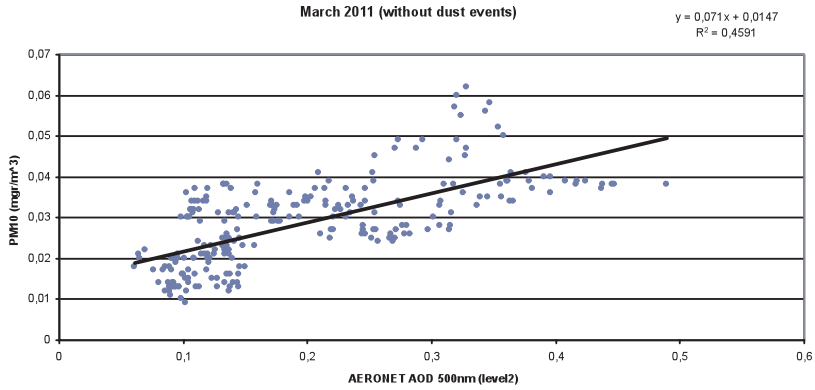

Figure 13: Correlation between PM10 and AERONET AOT for Limassol area after excluding days with dust layers (Nisantzi et al., 2011)

3.3 Field Spectroradiometric Measurements for Supporting AOT Image Based Values

The authors validated the AOT MODIS values through the use of field spectroradiometric measurements over standard calibration targets such as dark targets. GER1500 field spectroradiometers were used in this study to obtain spectral reflectances over dark targets in the area located near the Limassol Port (which is near the Limassol Castle) and nearby dark targets such as water dams in the District area of Limassol. (Figure 14).

To retrieve the AOT values from Landsat TM/ETM+, Themistocleous et al. (2011) developed a fast atmospheric correction based on the darkest pixel method using the MATLAB software to retrieve AOT through the radiative transfer (RT) equations. Themistocleous et al. (2011) used equation 1, based Gilabert et al. (1994) and Sifakis and Deschamps (1992) where

$$L_p = L_{pr} + L_{pa} \quad (1)$$

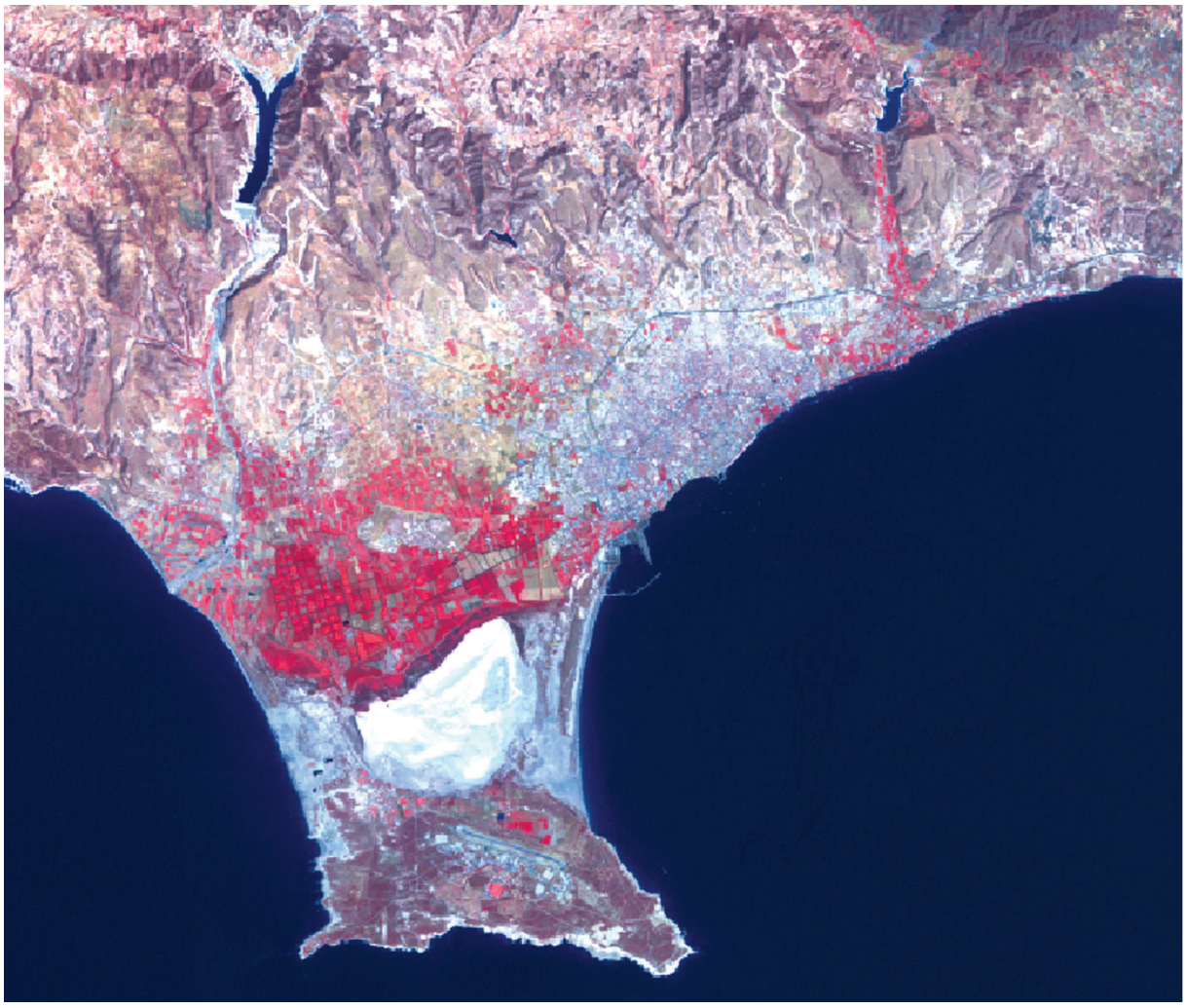

Figure 14: Landsat TM sub-scene over Limassol

where L_p = path radiance (measured in W/m2sr)
L_{pr} = atmospheric path radiance due to Rayleigh scattering in W/m^{2}sr
L_{pa} = atmospheric path radiance due to Mie scattering in W/m2sr.

The equations required to calculate atmospheric path radiance due to Rayleigh and Mie scattering are provided by Gilabert et al., (1994) and are well-known. The atmospheric path radiance (L_p) is calculated in equation 2 according to Hill and Sturm (1991) and Turner and Spencer (1972) which uses the satellite image radiance and reflectance values.

$$L_p = L_{ts} - \frac{\tau(\mu).\rho_{tg}.E_G}{\pi} \quad (2)$$

where
L_p = path radiance (integrated band radiance measured in W/m^{2}sr)
L_{ts} = at-satellite radiance measured in W/(m2 μm sr), as found from the satellite image
ρ_{tg} = target reflectance at ground level (in -situ measurement during satellite overpass) or the target reflectance value after applying the darkest pixel atmospheric correction method
E_G = global irradiance reaching the ground
$\tau(\mu)$ = direct (upward) target-sensor atmospheric transmittance.
E_G and $\tau(\mu)$ can be calculated as described by Hill and Sturm (1991).

Following, AOT was retrieved through equation 1, where it is an unknown value in the equation for Mie scattering (L_{pa}).

Figure 15: In situ spectroradiometric observations using the GER1500 field spectro-radiometer.

In-situ reflectance measurements were taken using a SVC HR 1024 spectroradiometer and AOT measurements were taken with the Cimel and Miscrotops sun-photometers (Figure 15). Following, the darkest pixel method of atmospheric correction was used to correct the satellite image from the effects of the atmosphere. Hadjimitsis et al. (2004a & 2004b) found that the darkest pixel atmospheric correction is the most effective atmospheric correction in the visible spectral bands.

The in-situ reflectance values from the reference target were compared with the reflectance value determined from the spectroradiometer. These values were inserted into the proposed algorithm in order to retrieve AOT. The AOT measurements retrieved were then compared with the in-situ measurements retrieved from the Microtops II and Cimel sun-photometers during the satellite overpass (Figure 16). Comparison of the AOT results obtained using this algorithm with the AOT values obtained from MODIS during the simultaneous overpass found a high correlation coefficient (R^2=0.87).

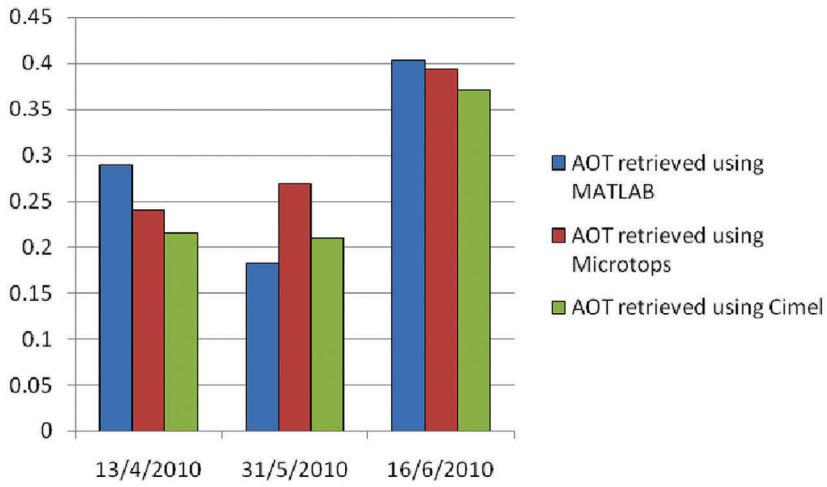

Figure 16. Comparison between AOT retrieved using the fast algorithm, AOT retrieved using Micrtops sunphotometer and AOT retrieved using the Cimel Sunphotometer (Themistocleous et al, 2011)

3.4 In situ Observations

In-situ observations were made at the Limassol Castle at Limassol to determine the deterioration of its construction materials. The deterioration resulted from air pollution in the area and other environmental conditions. Although the Limassol Castle is considered to be in good condition as a result of periodic maintenance, visual inspection indicates signs of decay, which are described as follows:

The deposition of air impurities on the surface of the material is a common phenomenon easily distinguishable with naked eye. These impurities create a form of incrustation adherent to the surface of the stone. Incrustations formed by polluted air present a dark gray to black colour (Figure 17). Furthermore, the prolonged exposure of a monument to inappropriate conditions can result in the loss of physical material, and degrade the material coherence (Figures 18 and 19). Other deterioration signs can be observed as the formation of honeycomb vacuum (Figure 20) or acupuncture corrosion (Figure 21).

Figure 17: Incrustation on the surface of limestone block.

Figure 18: Physical loss of material from the joints.

Figure 19: Physical loss of material from the surface of the block.

Figure 20: Honeycomb formation on the surface of the limestone block.

The 3D laser scanner Leica Scan Station C10 was used to document the Limassol castle (Figure 22). The specific laser scanner has a maximum scan rate of 50000 points per second, while the accuracy is ±6mm in position (X,Y,Z) at a distance up to 50m. The laser beam diameter is ±7mm, while the field of view of the Scan Station is 360o _ 270o. Moreover, the laser allows acquiring the reflected beam intensity and RGB colours. In order to monitor the effects of air pollution, the castle will be documented every year with the 3D laser

scanner. To establish that the deterioration is a result of air pollution, areas of the castle which show deterioration on the 3D laser scanner will have samples taken to determine the chemical analysis of the surface to establish if the deterioration was caused by air pollution or natural causes. Photographs of the castle were also taken and applied to the 3D laser scanned point cloud (Themistocleous et al., 2010)

In Figure 23, a sample of the point cloud is presented. As shown, intensity of laser is different in the joint sections and the deterioration

Figure 21: Acupuncture like corrosion on the surface of limestone block.

Figure 22: 3D laser scanning of the Castle and Point cloud generated by 3D laser scanner

signs of the monuments which were also verified with in situ observations.

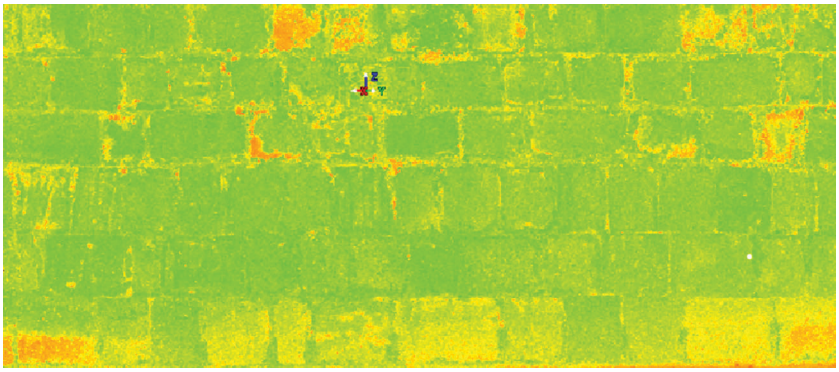

Figure 23: Point cloud generated by 3D laser scanner.

4. CONCLUSIONS

Air pollution can be a significant factor contributing to damage of cultural heritage sites, as indicated by signs of deterioration on the building. Continuous measure of air pollution around cultural heritage sites can assist local decision makers to take appropriate measures to improve air quality, which will assist in conservation of monuments and cultural heritage sites and prevent further damage. Therefore, by improving air quality, the local authorities and government agencies will be able decelerate the decay of our cultural heritage.

Remote sensing is an excellent tool to monitor and document the effects of air pollution on monuments and cultural heritage sites. This study examined open air monuments in the four major cities in Cyprus and provided a case study of the Limassol Castle. By using a variety of tools, including satellite images, sun-photometers, PM10 monitors, and laser scanners, the level of air pollution and its effect on cultural heritage sites can be determined. Finally, GIS was used to map the monuments examined in this paper and map any significant areas of pollution, including urban areas, industrial areas, and roads. In the future, the GIS database will be extended to include all the visible open to air monuments. The methodology presented in this study can be implemented anywhere in the world to monitor the impact of air pollution on cultural heritage sites. Future work can utilize archive satellite data to create a digital database in order to examine the long term distribution of air pollutants at such sites. The algorithm proposed by Themistocleous (2011) can also be used with archived satellite images in order to identify pollution levels and trends in targeted areas. Identifying air pollution trends will assist in policy planning to minimize air pollution, especially in major cities.

Acknowledgements

The authors would like to express their acknowledgments to Cyprus University of Technology -Research Committee, ("Monitoring" project) and to Cyprus Research Promotion Foundation ("AirSpace" project). Partial work presented in this study (spectro-radiometric measurements and atmospheric correction) is part of Kyriacos Themistocleous's PhD thesis entitled "Improving atmospheric correction methods for aerosol optical thickness retrieval supported by in-situ observations and GIS analysis".

References from Journals:

Ferradás, G. E., (et al.), 2010. An approach for determining air pollution monitoring sites. *Atmospheric Environment*, 44(21-22), pp. 2640-2645.

Ghedini, N., (et al.), 2011. Atmospheric aerosol monitoring as a strategy for the preventive conservation of urban monumental heritage: The Florence Baptistery. *Atmospheric Environment*, 45(33), pp. 5979-5987.

Gilabert, M.A., Conese, C., and Maselli, F., (1994). An atmospheric correction method for the automatic retrieval of surface reflectances from TM images.*, Intl Jour. of Rem. Sens,* 15(10), pp. 2065–2086.

Hadjimitsis, D.G. (et al.), 2004a. An assessment of the effectiveness of atmospheric correction algorithms through the remote sensing of some reservoirs. *Intl Jour. of Rem. Sens.*, 25(18), pp. 3651–3674 .

Hadjimitsis, D. G., 2008. Description of a New Method for Retrieving the Aerosol Optical Thickness from Satellite Remotely Sensed Imagery Using the Maximum Contrast Value and Darkest Pixel Approach. *Transactions in GIS*, 12: pp. 633–644. doi: 10.1111/j.1467-9671.2008.01121.x

Hadjimitsis D.G., and. Clayton C.R.I., 2009. Determination of aerosol optical thickness through the derivation of an atmospheric correction for Landsat TM band 1 image data: an application to areas located in the vicinity of airports at UK and Cyprus, *Applied Geomatics Journal,* 1(2), pp.31-40 doi: 10.1007/s12518-009-0004-2.

Hadjimitsis, D.G., 2009. Aerosol optical thickness (AOT) retrieval over land using satellite image-based algorithm, *Air Quality, Atmosphere & Health- An International Journal,* 2 (2), pp. 89-97 DOI 10.1007/S11869-009-0036-0

Hill, J., and Sturm, B., 1991. Radiometric correction of multi-temporal Thematic Mapper data for use in agricultural land cover classification and vegetation monitoring, *Intl Jour. of Rem. Sens.,* 12(7), pp. 1471-1491.

Holben, B.N., (et al.), 1998. AERONET – A federated instrument network and data archive for aerosol characterization. *Rem. Sens. Environ.*, 66, pp. 1-16.

Kaufman, Y.J. (et al.), 1997. Operational remote sensing of tropospheric aerosol over the land from EOS-MODIS, *Journal of Geophysical Research*, 102, pp. 17051–17068.

Lee, H. J. (et al.), 2011. A novel calibration approach of MODIS AOD data to predict PM2.5 concentrations, Atmos. Chem. Phys., 11, pp. 7991-8002, doi:10.5194/acp-11-7991-2011.

Martin, V. R., 2008. Satellite remote sensing of surface air quality. *Atmospheric Environment,* 42(34), pp. 7823-7843.

Nava, S. (et al.), 2010. An integrated approach to assess air pollution threats to

cultural heritage in a semi-confined environment: The case study of Michelozzo's Courtyard in Florence (Italy). *Science of The Total Environment*. 408(6), pp. 1403-1413.

Péré, J.C., (et al.) 2009. Mapping of PM10 surface concentrations derived from satellite observations of aerosol optical thickness over South-Eastern France. *Atmospheric Research,* 91(1), pp. 1-8

Pfeffer, H.U. (et al.), 1995. Air pollution monitoring in street canyons in North Rhine-Westphalia, Germany. *Science of The Total Environment,* 169(1-3), pp. 7-15.

Pujadas, M., 2000. Passive remote sensing of nitrogen dioxide as a tool for tracking air pollution in urban areas: the Madrid urban plume, a case of study. *Atmospheric Environment,* 34(19), pp. 3041-3056.

Pummakarnchana, O. (et al.), 2005. Air pollution monitoring and GIS modeling: a new use of nanotechnology based solid state gas sensors, *Science and Technology of Advanced Materials.* 6(3-4), pp. 251-255.

Retalis, A. (et al), 2010. Comparison between visibility measurements obtained from satellites and ground, *Natural Hazards and Earth System Sciences Journal*. 10(3) pp. 421-428 (2010) doi:10.5194/nhess-10-421-2010.

Sifakis, N., and Deschamps, P.Y., (1992). Mapping of air pollution using SPOT satellite data. *Photogr.Eng.and Rem. Sens.,* 58, pp. 1433-1437

Tømmervik, H., 1995. Monitoring the effects of air pollution on terrestrial ecosystems in Varanger (Norway) and Nikel-Pechenga (Russia) using remote sensing. *Science of The Total Environment,* 160-161, pp. 753-767.

References from Proceedings and Books:

Hadjimitsis, D. G., (et al.), 2010. *Satellite remote sensing, GIS and sun-photometers for monitoring PM10 in Cyprus: issues on public health*. R.Meynert, S.P. Neeck and H. Shimonda (eds.) Proc. SPIE 7826, 78262C, doi:10.1117/12.865120

Hadjimitsis, D.G. (et al.), 2004b. *On the darkest pixel atmospheric correction algorithm: a revised procedure applied over satellite remotely sensed images intended for environmental applications.* M. Ehlers, H.J. Kaufmann, and U. Michel (eds.) Proc. SPIE 5239, 464; doi:10.1117/12.511520.

Kozaris, G., and Kefalas, M., 1989. *Effects of air pollution on marble monuments. The role of acid rain,* Thessaloniki. (in greek).

Nisantzi, A. (et al.), 2011. *Estimating the relationship between aerosol optical thickness and PM10 using lidar and meteorological data in Limassol, Cyprus, U.N. Singh and G. Pappalardo (eds.)* U.N. Singh and G. Pappalardo (eds. Proc.. SPIE 8182, 818217 , doi. 10.1117/12.898357.

Reyes, J., (et al.), 2011. *Influence of Air Pollution on Degradation of Historic Buildings at the Urban Tropical Atmosphere of San Francisco*. Chmielewski G. A. (ed.), Monitoring, Control and Effects of Air Pollution, In Tech (open access), 201 – 226

Skoulikides, N.T., 2000 *Corrosion and maintenance of construction materials of monuments,* Heraklion (in greek).

Themistocleous, K., (et al.), 2010. *Monitoring Air Pollution in the Vicinity of Cultural Heritage Sites in Cyprus Using Remote Sensing Techniques,* Digital Heritage, Lecture Notes in Computer Science, 2010, Vol. 6436/2010, 536-547, DOI: 10.1007/978-3-642-16873-4_44. M. Ioannides (ed.): EuroMed 2010, LNCS 6436, pp. 536–547, 2010, Springer-Verlag Berlin Heidelberg 2010.

Themistocleous, K., (et al.), 2011. *Fast atmospheric correction algorithm based on the darkest pixel approach for retrieving the aerosol optical thickness: comparison with in-situ AOT measurements,E.I. Kassianov, A. Comeron, R.H. Picard, and K. Schafer (eds),* SPIE 8177, 81770B, doi. 10.1117/12.898593.

Turner, R.E., and Spencer, M.M, (1972). Atmospheric model for correction of spacecraft data. *Proc. Eight International Symposium on Remote Sensing of the Environment, II.,* pp. 895-934.

References from Other Literature:

Tsanev, V. I., and Mather, T. A., 2008. Microtops Inverse Software package for retrieving aerosol columnar size diustributions using Microtops II data", Users Manual (2008).